

# Anti-Deceptive Jamming and Target Detection with Non-Linear FDA-MIMO Radar

Abdul WAHAB<sup>a,1</sup>, Kashif HUSSAIN<sup>a</sup>, Naila SHAHEEN<sup>a</sup>, Raza KHAN<sup>b</sup>

<sup>a</sup> Frankfurt University of Applied Sciences, Frankfurt, Germany

<sup>b</sup> School of Electrical Engineering, International Islamic University, Islamabad, Pakistan

**Abstract.** FDA-MIMO radar is a new form of radar technology that has a vast range of applications. Jamming is one of the many issues faced by the FDA-MIMO radar, such as deceptive jamming and target detection. A lot of work has been done in the fields of jamming and anti-jamming with FDA-MIMO radar. This paper introduces a non-linear SMA-FDA MIMO radar. Modified SMA has been proposed and implemented, which was never used in the radar application before it was used in the biological fields. Anti-deceptive jamming has been performed over the FDA-MIMO. Desired targets are being detected successfully. Simulation results are presented to show the efficiency of the proposed algorithm.

**Keywords.** Frequency diverse array radar, anti-deceptive jamming, target detection, parameter estimation

## 1. Introduction

Frequency diverse array radar has been a hot research topic in the recent decade. Antonick et al. [1], [2] first proposed a frequency diverse array (FDA). Since then, FDA has been studied in different aspects, including transmit beam pattern [3], array configuration design [4], [5], parameter estimation [6], [7], [8], moving target indication (MTI) [9], clutter suppression [10], [11], and interference mitigation [12]. FDA uses tiny frequency increments across array elements. The frequency increment is tiny and minimal compared to the carrier frequency and bandwidth. Due to the modest frequency increment, another degree of freedom (DOF) can be leveraged, making the beam pattern a function of range, angle, and time. Such an angle-range-dependent beam pattern has numerous intriguing applications, including synthetic aperture radar (SAR) and moving target indication [13], [14]. FDA can detect and localize targets by reducing range ambiguity using a single pulse repetition frequency. The frequency offset among FDA elements improves FDA radar performance by regulating range-angle dependency and spatial beam pattern dispersion [15]. Researchers are interested in finding the optimal frequency offset between adjacent linear FDA elements to boost performance. [16] Proposed an FDA with an adaptive frequency offset selection approach to enhance SINR.

---

<sup>1</sup> Corresponding Author, Abdul Wahab, Frankfurt University of Applied Sciences, Frankfurt, Germany ; E-mail: wahab.engr55@yahoo.com.

FDA-MIMO radar with a time-dependent frequency offset to improve time-dependent beam pattern for a given target range and orientation. Non-uniform antenna offsets were used to find novel FDA radar characteristics. Sub-array FDA in [17] helps estimate target placements by employing beam space-based MUSIC. [18] Studied avoiding deceptive jamming to discern true and false targets with MIMO-FDA. Later a novel strategy in [16] Suggested jointly estimating target range and angle by using an appropriate frequency offset for MIMO FDA to improve range angle beam pattern for better detection and estimation. SA-FDA MIMO [2] radar to suppress main-beam jamming. They first utilize simulated annealing to calculate FDA frequency increases. Its beam pattern is single peak decoupled, unlike the typical FDA beam pattern. Second, non-linear frequency increases make erroneous target echoes distinct in the power spectrum. Adaptively filtered echoes suppress false main-beam jamming while retaining target signals. Simulations show that the proposed strategy can suppress main-beam deceptive jamming. When the radar functions, the environment changes constantly and target information is unavailable. The transmitter illuminates the radar environment, then the reception systems adaptively sense the environment by detecting the radar returns to gain target information. This is feedback from receive to transmit systems. The broadcast and receive systems alter their parameters with feedback. Iterative optimization techniques can use feedback to calculate optimal transmitting and receiving beamforming parameters. The fake target generator uses time-delay modulation to provide longer-lasting signals than the current pulse period (pulse repetition intervals). The radar picks up false positives before, after, and in place of the target. Thus, the radar follows fictional targets. It's a form of radar jamming because it consumes radar power and slows detection. The current pulse period is shorter than the target delays. By adjusting the time delay's amplitude, we may make the bogus target seem ahead in case 1 or behind in case 2. So, the linear FDA MIMO radar has concerns such as angle estimation, parameter estimation, optimization problems, and poor performance against jamming signals. In this article, we used SMA-FDA MIMO radar to alleviate issues with traditional FDA MIMO radar. SMA-FDA MIMO is a novel development in nonlinear FDA MIMO radar. The standard FDA MIMO radar's parameter estimation, optimization, and anti-jamming performance are all improved.

## 2. SMA-FDA MIMO Radar Signal Model

### 2.1. System Model

Since the drawbacks of the traditional and linear FDA-MIMO system under main-beam misleading jamming, non-linear FDA-MIMO is becoming popular. How to select the non-linear frequency offset,  $f_m$ ,  $m = 0, 1, \dots, M-1$ , is a research question. Several methods to design nonlinearly increased frequencies have been proposed, including the logarithmically increasing frequency offset [1], the random offset [4], genetic algorithm-based optimization [6], particle swarm optimization [2], subarray-based FDA framework [7], and Taylor windowed frequency offsets [3]. In this paper, we have proposed to apply the SMA to FDA MIMO to pick non-linear radar frequency increments. [2] Employs the simulated annealing (SA) approach to achieve non-linear FDA MIMO radar frequency increases. The best-N p population from SMA-FDA-MIMO can also be used for target detection and classification. After detecting the target range and slant angle, ( $R_0$  and  $\Psi_0$ )

, range-angle matching filtering weight can be solved by using a conventional minimal variance distortion-less response (MVDR) adaptive beam shaper. The whole form of the expression is as follows,  $\min_w w^H R w$  subject to:  $w^H s(R_0, \Psi_0) = 1$ , where  $w$  is the range-angle matching filtering weight,  $R$  is the covariance matrix of the jamming and noise signal after subtracting the target signal, and  $(R_0, \Psi_0)$  is the pointing vector for the target's range and slant angle.  $s(R_0, \Psi_0) = \vec{a}_t(\Phi_{d;\psi_0}) \otimes \vec{a}_r(\Phi_{d;\psi_0})$ . By using adaptive filtering, FDA-MIMO radar can suppress spurious targets in the transmission angular frequency domain. In the above adaptive filtering, estimating the covariance matrix of the jamming and noise signal is problematic, especially when acquiring independent and identically distributed snapshots in real-time and when subspace leaking dominates the Eigen spectrum of the covariance matrix. This research focuses on improving covariance matrix estimation to boost system performance and robustness. Slime mold algorithm SMA [19] is a population-based optimizer based on slime mold in nature. SMA provides a unique mathematical model, competitive outcomes, and fast convergence for many problems, notably real-world instances. The gradient-free SMA approach simulates slime mold wave feedback. Dynamic structure with a balance between global and local search drifts. Many scholars have applied this strategy to real-world situations and published their results in top international journals. . The proposed SMA process is as follows:

**Algorithm : Procedure of SMA-FDA-MIMO**

[1] Given  $\Delta f_{min}, \Delta f_{max}$  as the allowed minimum and maximum frequency increment between two elements,

[2] Give  $P$  as the size of the population

[3] Let  $T$  be the maximum number of the epochs to iterate

[4] Initialize the population at  $t = 0$  as  $X_1, X_2, \dots, X_P$ , where  $X_i \in \mathbf{U}[\Delta f_{min} \Delta f_{max}]^M$

[5] for  $t \leftarrow 1, T$

[5.1] Update the population as follows:

$$X(t+1) = \begin{cases} rand(UB - LB) + LB & rand < z \\ X_b(t) + v_b(WX_A(t) - X_B(t)) & r < p \\ v_c X(t) & r \geq p \end{cases}$$

Where the meanings of  $v_b, v_c, X_b, X_A, X_B, r, p, z, UB, LB, W$  can be referred to [1].

[5.2] Calculate the evaluation values  $V_1, V_2, \dots, V_P$  corresponding to every  $X_i$  in the population.

[5.3] Save the best evaluation value  $V_b(t)$  and  $X_b(t)$

[5.4] end for

Above, we used the same formula as in [2] to derive the evaluation value  $V_i(t)$ : Give  $X_i = [\Delta f_1, \Delta f_2, \dots, \Delta f_M]^T$ , gain  $g(\psi, r)$  is the square of the region beam pattern gain outside the desired position (denoted as  $g(\psi_{D^-}, r_{D^-})$ ) minus the square of the region beam pattern gain within the desired position (denoted as  $g(\psi_D, r_D)$ ), namely  $g(\psi, r) = g(\psi_{D^-}, r_{D^-}) - g(\psi_D, r_D)$ . The evaluation value  $V_i(t) = 1/g(\psi, r)$ . A set of  $X_b$  values obtained from the algorithm [4] are put into the non-linear FDA MIMO radar. The non-linear FDA MIMO radar is fed with a series of  $X_b$  values calculated using the algorithm [4]. Figure 1 below depicts the geometry of the SMA-FDA MIMO radar as well as the radar signal format.

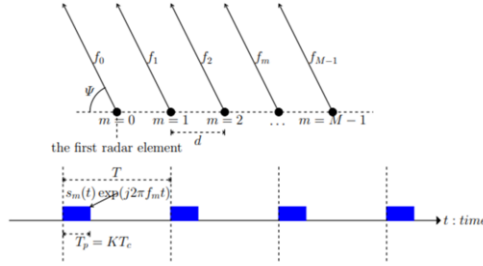


**Figure 1.** The geometry of SMA-FDA MIMO radar and signal format

Figure 1 shows an antenna array with  $M$  radar elements. Array spacing is  $d$ . The pulse repetition frequency  $f_{PRF} = \frac{1}{T}$ . is equal to  $1/T$ , and it is transmitted in a synchronized fashion from each radar element in the array. The radar's carrier frequency,  $f_c$ , provides the basis for all transmissions, but the frequency of the signal broadcast by each antenna element is shifted by an amount, or "offset," from the carrier frequency, as shown by the expression,

$$f_m = f_c + \Delta f_m, \quad m = 0, 1, 2, \dots, M - 1 \quad (1)$$

Where we have  $\Delta f_m$  is the frequency offset of the  $m$ -th antenna element relative to  $f_c$ . In a practical radar system, it always has:

$$\Delta f_m \ll f_c \quad (2)$$

The signal from  $m$ -th antenna element is,

$$x_m(t) = \text{rect}\left[\frac{t}{T_p}\right] s_m(t) \exp(j2\pi f_m t), \quad m = 0, 1, 2, \dots, M - 1 \quad (3)$$

Where  $\text{rect}\left[\frac{t}{T_p}\right]$  is a rectangular signal pulse with the width equal to  $T_p$ ; and  $s_m(t)$  is the orthogonal waveform with a cyclic prefix (CP) length ( $\tau_{CP}$ ) transmitted in the  $m$ -th antenna element, i.e.,

$$\int_{t=\tau_{CP}}^{T_p} s_i(t) s_j^*(t) dt = \begin{cases} 1 & i = j \\ 0 & i \neq j \end{cases} \quad (4)$$

$$\int_{t=\tau_{CP}}^{T_p} s_i(t) s_i^*(t - kT_c) dt = \begin{cases} 1 & k = 0 \\ 0 & k = 1, 2, \dots, K - 1 \end{cases}$$

Where  $T_c$  is the sampling chip rate, and  $K = \frac{T_p}{T_c}$ . Far-field target  $P$  is at  $(R_0, \Psi_0)$  where  $R_0$  is the slant range and  $\Psi_0$  is the slant angle between the first antenna element and the far field target  $P$ . Once the  $m$ th antenna element's signal reaches  $P$ , it becomes;

$$\hat{x}_m(t) = \text{rect}\left[\frac{t - \frac{\tau_{R_0}}{2} - \tau_{dm}}{T_p}\right] s_m\left(t - \frac{\tau_{R_0}}{2} - \tau_{dm}\right) \exp(j2\pi f_m (t - \frac{\tau_{R_0}}{2} - \tau_{dm})) \quad (5)$$

Here  $\tau_R = \frac{2R_0}{c}$  is the two-way propagation delay from the first radar element to target  $P$ ;  $\tau_{dm} = \frac{m d \cos \Psi_0}{c}$  is the delay difference between the  $m$ -th and first radar elements when target  $P$  is at angle  $\Psi_0$  relative to the first radar element. Assume  $N$  radar elements in the transmitting array. In this article, only monostatic radar is examined, therefore the transmitting and receiving arrays have the same element space  $d$  and number of radar

elements,  $N=M$ . After the target  $P$  reflects the signal  $\hat{x}_m(t)$  ( $m = 0, 1, \dots, M - 1$ ), the  $n$ -th radar element receives its echo.

$$\tilde{x}_n(t) = \check{\rho}_0 \sum_{m=0}^{M-1} \left\{ \text{rect} \left[ \frac{t - \tau_{R_0} - \tau_{dm} - \tau_{dn}}{\tau_p} \right] s_m(t - \tau_{R_0} - \tau_{dm} - \tau_{dn}) \right. \\ \left. \exp(j2\pi f_m(t - \tau_{R_0} - \tau_{dm} - \tau_{dn})) \right\} \quad (6)$$

When calculating the delay between the  $n$ th receiving element and the reference element, we use the formula  $\tau_{dn} = \frac{nd\cos\Psi_0}{c}$ , where  $\check{\rho}_0$  is the propagation gain and scattering coefficient at the target  $P$ . The received signal in each radar element is then filtered through the Array Signal Processing Module as depicted in Fig 2. The cyclic prefix of  $s_m(t)$  is selected to satisfy,

$$\tau_{dm} + \tau_{dn} < \tau_{CP} \quad (7)$$

i.e., the aggregated delay difference is less than the length of the cyclic prefix of the orthogonal waveform, so that the orthogonality between any pair of  $s_m(t)$  is preserved.

In the array signal processing module, the signal from each receiving radar element will be matching-filtered in  $M$  channels, each of the channels is a maximum ratio match filter with its coefficients equal to  $s_m^*(t - \tau_R)$ , i.e., The  $m$ th transmitting radar element's waveform is the conjugate transposition of the orthogonal waveform with a delay of  $\tau_R = \frac{2R}{c}$ . After the matched filtering, the signal is down-converted by  $\exp(j2\pi f_m t)$ , the output from the array signal processing module at time  $= \tau_R$  is a matrix  $X = [x_{m,n}(R; \Psi_0)]$ ,  $m = 0, 1, \dots, M - 1$  and  $n = 0, 1, \dots, N - 1$ , where,

$$x_{m,n}(R; \Psi_0) = \rho_0(R) \exp \left\{ j2\pi f_m \left( -\frac{2R_0 - 2R}{c} - \frac{md\cos\Psi_0}{c} - \frac{nd\cos\Psi_0}{c} \right) \right\} \quad (8)$$

When  $\rho_0(R)$  is the product of  $\check{\rho}_0$  and the gain from the match filter at delay  $\tau_R$ . By substituting  $f_m = (f_c + \Delta f_m)$  and using the approximation that  $\Delta f_m \ll f_c$ , the expression of  $x_{m,n}$  can be simplified as [2]:

$$x_{m,n}(R; \Psi_0) \approx Y_0 \rho_0(R) \exp \left\{ j2\pi \left[ -\Delta f_m \frac{2R_0 - 2R}{c} - f_c \left( \frac{md\cos\Psi_0}{c} + \frac{nd\cos\Psi_0}{c} \right) \right] \right\} \quad (9)$$

Where,  $Y_0 = \exp[-j2\pi f_c \frac{2R_0 - 2R}{c}]$  and  $X$  can be symbolized in the matrix form as,

$$\mathbf{X}(R, \Psi_0) = Y_0 \rho_0(R) (\text{diag}[\vec{\mathbf{a}}_{f_{da}}(\overline{\Delta\Phi_{R_0-R}})]) (\vec{\mathbf{a}}_t(\Phi_{d;\Psi_0})) (\vec{\mathbf{b}}_r(\Phi_{d;\Psi_0}))^T \quad (10)$$

Where,  $[\cdot]^T$  is the matrix transpose operation;  $\overline{\Delta\Phi_{R_0-R}} = \frac{2R_0 - 2R}{c} [\Delta f_0, \Delta f_1, \dots, \Delta f_{M-1}]^T$ ,  $\Phi_{d;\Psi_0} = \frac{f_c d \cos\Psi_0}{c}$ , and

$$\vec{\mathbf{a}}_{f_{da}}(\overline{\Delta\Phi_{R_0-R}}) = [\exp(-j2\pi \frac{(2R_0 - 2R)\Delta f_0}{c}), \exp(-j2\pi \frac{(2R_0 - 2R)\Delta f_1}{c}), \dots, \exp(-j2\pi \frac{(2R_0 - 2R)\Delta f_{M-1}}{c})]^T$$

$$\vec{\mathbf{a}}_t(\Phi_{d;\Psi_0}) = [1, (\exp(-j2\pi\Phi_{d;\Psi_0}))^1, \dots, (\exp(-j2\pi\Phi_{d;\Psi_0}))^{M-1}]^T$$

$$\vec{\mathbf{b}}_r(\Phi_{d;\Psi_0}) = [1, (\exp(-j2\pi\Phi_{d;\Psi_0}))^1, \dots, (\exp(-j2\pi\Phi_{d;\Psi_0}))^{N-1}]^T \quad (11)$$

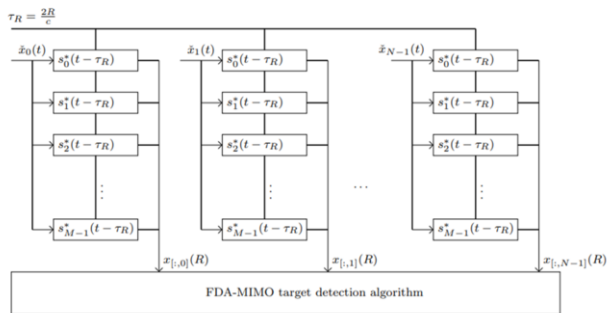


Figure 2. Array Signal Processing Module

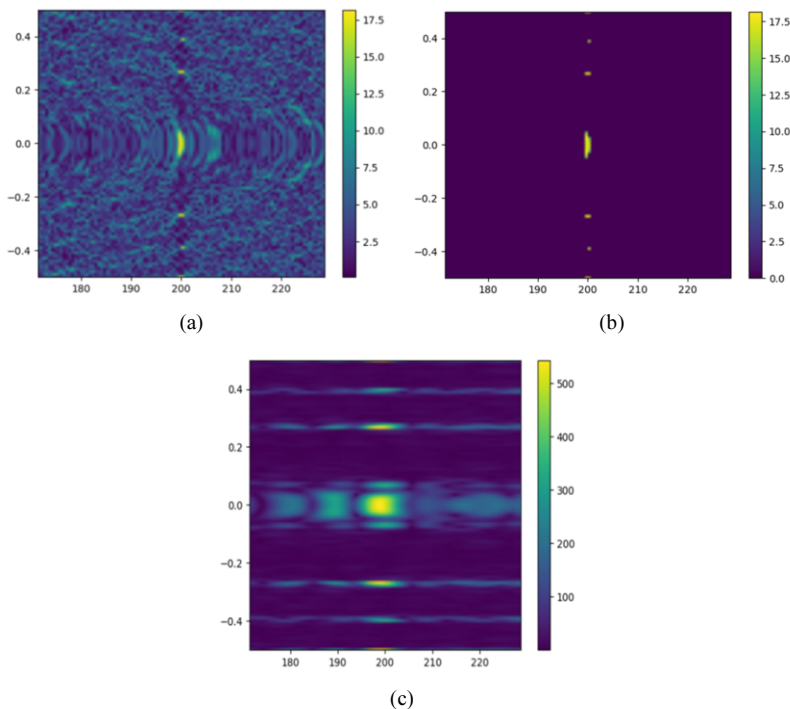


Figure 3 (a), (b) & (c) FDA-MIMO radar target detection in different ranges

However, because of the orthogonality of the waveform  $s_m(t)$ , the match filter can only have its output maximized, when  $\tau_R = \tau_{R_0}$ , i.e.  $\rho_0(R) = |\rho_0| \exp(-j\beta_0) \delta(R - R_0)$ , where;

$$\delta(R - R_0) = \begin{cases} 1 & R = R_0 \\ 0 & R \neq R_0 \end{cases} \quad (12)$$

And  $|\rho_0| \exp(-j\beta_0)$  is the product of the maximum gain  $|\rho_0|$  along with a phase rotation of  $\exp(-j\beta_0)$ , The target detection for different ranges are given in the figure 3

(a) and (b) below, when it is synchronized, and the output from the array signal processing module is;

$$\mathbf{X}(R; \Psi_0) = |\rho_0| \exp(-j\beta_0) \delta(R - R_0) (\vec{\mathbf{a}}_t(\Phi_d, \Psi_0)) (\vec{\mathbf{b}}_r(\Phi_d, \Psi_0))^T \quad (13)$$

### 3. SMA-FDA MIMO Radar Jamming Signal Model

False target generators provide the jamming signal by sending the radar false target parameters, causing it to lose track of the real target. Assume that the  $j$ -th ( $j=1,2,\dots$ ) false target is located at coordinates  $(R_j, \Psi_j)$ , where  $R_j$  is the equivalent slant range of the  $j$ -th false target generator given the transmission delay of  $R_0$  plus the extra delay ( $\Delta_\tau$ ) in the caching-and-retransmitting method.. The equivalent delay,  $\tau_{R_j}$  is expressed as

$$\tau_{R_j} = \frac{R_j}{c} = \frac{R_0}{c} + \Delta_\tau = \tau_{R_0} + \Delta_\tau \quad (14)$$

The  $j$ -th false target's slant angle is denoted by  $\Psi_j$ . This article solely takes into account false jamming signals at main-beam range, so that  $\Psi_j = \Psi_0$ . which is in line with the actual target angle. The received signal by the  $n$ -th radar element that is echoed by the  $j$ -th false target generator is;

$$\check{p}_{n,j}(t) = \check{\rho}_{n,j} \sum_{m=0}^{M-1} \text{rect}\left[\frac{t - \tau_{R_j} - \tau_{dm} - \tau_{dn}}{T_p}\right] s_m(t - \tau_{R_j} - \tau_{dm} - \tau_{dn}) \exp(j2\pi f_m(t - \tau_{R_j} - \tau_{dm} - \tau_{dn})) \quad (15)$$

Depending on the range of the  $R_j$ , the delayed signal,  $\check{p}_{n,j}(t)$ , may fall out of current detection window  $[0, T_p]$ , where  $T_p = \frac{1}{f_{PRE}}$ , that is, when  $\frac{2R_j}{c} > T_p = \frac{1}{f_{PRE}}$ , i.e.,  $R_j > \frac{c}{2f_{PRE}}$ , then the delayed signal will fall into the next detection windows and cause jamming.  $R_u = \frac{c}{2f_{PRE}}$  is defined as the largest possible interval without introducing any ambiguity. Vice versa, in the current detection window from  $[0, T_p]$ , where,  $T_p = \frac{1}{f_{PRE}}$ , there will be other jamming falling from previous detection windows, with an equivalent position at  $R'_j = R_j - u * R_u$ , where  $u$  is the largest non-negative integer satisfying that  $0 < R'_j < R_u$ . Note that  $R'_j$  may be smaller than  $R_0$ , i.e., the range of the true target. Hence,  $R_j$  will be used instead of  $R'_j$  for more brevity with no ambiguity. After the Array Signal Processing Module, the received jamming signal from the  $j$ -th false target after the demodulation at delay  $\tau_R$  can be approximated by a signal matrix,  $P_j = [p_{m,n,j}(R; \Psi_j)]$ , as shown in the fig 4 (a) shows the normalized frequency spectrum while (b) depicts the suppression performed by the FDA-MIMO radar and (b) shows the suppression performed by the SMA-FDA MIMO radar ,which clear shows the performance improved with better suppression where;

$$P_{m,n,j}(R; \Psi_j) = Y_j \rho_j(R) \exp\left\{j2\pi\left[-\Delta f_m \frac{(2R_j - 2R)}{c} + \Delta f_m \Delta_\tau - f_c \left(\frac{m d \cos \Psi_j}{c} + \frac{n d \cos \Psi_j}{c}\right)\right]\right\} \quad (16)$$

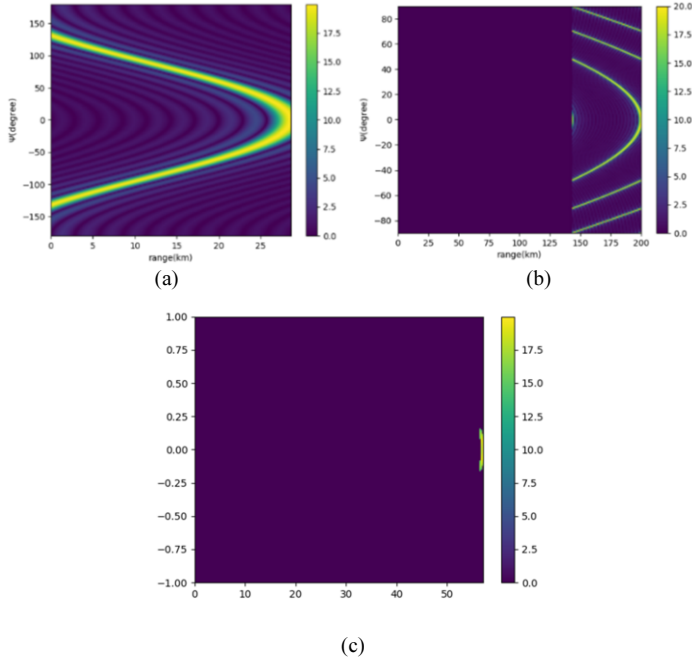


**Figure 4.** Transmit pattern (a) Normalized frequency spectrum, (b) FDA-MIMO (b) SMA-FDA MIMO

Where  $\Upsilon_j = \exp\left[-j2\pi f_c \frac{2R_j - 2R_0}{c}\right]$ ,  $\rho_j$  false target scattering coefficient, propagation gain, match filter gain. When compared to Eq.8, the Eq.16 has a phase discontinuity,  $\Delta f_m \Delta \tau$ . This phase discontinuity is due to the additional delay  $\Delta \tau = \frac{2R_j - 2R_0}{c}$  during the caching-and-retransmit procedure in the  $j$ -th false target generator. Such a delay can't be fully compensated in the down conversion because, when the signal from the false target is reflected by cached-and-retransmission procedure, its phase rotation is paused. In contrast, if the signal is really in transmission, its phase will be rotating all the time. In the similar way as in the match filtering of  $\mathbf{X}$ , the gain from the matching filter can be maximized only when  $R = R_j$ , i.e.  $\rho_j(R) = |\rho_j| \exp(-j\beta_j) \delta(R - R_j)$ . So the output from the demodulator for the  $j$ -th false target signal can be simplified in the matrix form as;

$$\mathbf{P}_j(R; \Psi_j) = |\rho_j| \exp(-j\beta_j) \delta(R - R_j) \left( \text{diag} \left[ \overline{\mathbf{a}_{fda}(\Delta \Phi_{R_j - R_0})} \right] \right) \left( \mathbf{a}_t(\Phi_{d, \Psi_j}) \right) \left( \mathbf{b}_r(\Phi_{d, \Psi_j}) \right)^T \quad (17)$$

Where,  $[\cdot]^T$  is the vector transpose operation;  $\overline{\Delta \Phi_{R_j - R_0}} = \frac{2R_j - 2R_0}{c} [\Delta f_0, \Delta f_1, \dots, \Delta f_{M-1}]^T$ .

After combining the signal from the true target at  $R_0$  and the false targets at  $R_j$ ,  $j = 1, 2, \dots, J$ , the aggregated signal is denoted by a matrix  $\mathbf{Y}$  defined as

$$\mathbf{Y}(R; \Psi_0, \Psi_{j=1, \dots, J}) = \mathbf{X}(R; \Psi_0) + \sum_{j=1}^J \mathbf{P}_j(R; \Psi_j) + \mathbf{N}_o \quad (18)$$

Where  $\mathbf{N}_o = [n_{m,n}]$  is a matrix of Gaussian white noise with  $n_{m,n} \sim \mathcal{N}(0, \sigma^2)$ .

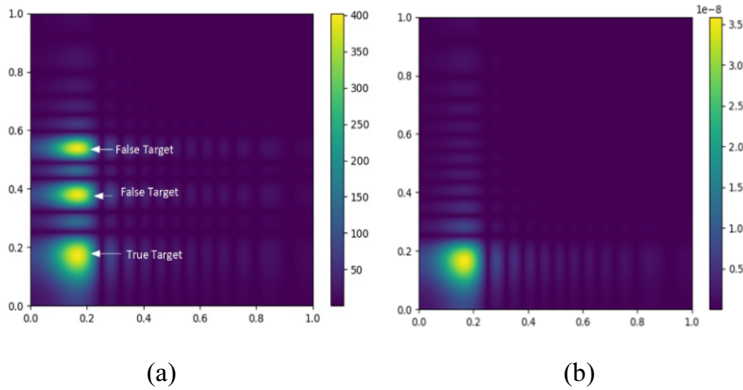


**Figure 5.** Jamming suppression With (a) FDA-MIMO (b) SMA-FDA MIMO

To examine design and signal processing issues. Using a non-regular frequency increment and array arrangement can achieve range-angle focusing in FDA's beam pattern at a given time, however it causes energy dispersion. However you can see in the fig 5(a) that FDA-MIMO radar the deceptive jamming suppression is very poor and in fig 5 (b) SMA-FDA MIMO radar which clearly shows better performance than the traditional FDA-MIMO radar. The time-variant beam pattern complicates target localization and other applications. Ideal orthogonal waveforms are not accessible for non-linearly increasing FDA-MIMO, hence waveform design and optimization is required. The waveform design purpose is similar to MIMO radar, but the optimization methods differ due to frequency increase. FDA-MIMO radar can tackle the main lobe jamming suppression problem, a bottleneck in traditional radar, utilizing a jamming suppression technique. Practical issues like as pseudo-random distance distribution and coherent repeater jamming should be considered. Non-ideal orthogonality should be considered when implementing a non-linear FDA-MIMO system. Each antenna element's individual frequency inaccuracy will reduce coherent demodulation performance. Parallel calculation for SMA can also speed up FDA-MIMO radar synthesis. FDA-MIMO radar has been studied for decades, but non-linear FDA-MIMO radar is just becoming popular due to large-scale, sophisticated computations. The linear FDA-MIMO system analysis is mature and can be used in the non-linear analysis.

#### 4. Conclusion

We introduce the SMA-FDA MIMO radar system and offer a anti-deceptive jamming approach for main-beam range attacks. First, annealing optimizes non-linear frequency increments, resulting in a unidirectional, single-point decoupled radar beam pattern. In the normal FDA S-shaped beam pattern, the primary beam's high gain zone is limited by pulse width. Despite varying pulse widths, the beam's angular directivity stays constant. The SMA-FDA-MIMO radar has multiple delay range zones, and spurious target echoes vary between them. Signal fine-tuning can achieve the same signal gain as typical MIMO radar in non-delay range. The fake signals have a discontinuous distribution pattern and low gain, while the target signal is continuous and strong. By adapting range and angle, we can shield the genuine target signal from main-beam range jamming. Results show

the approach's better performance and versatility. This method can be applied with many array geometries. Future research could improve the precision with which target parameters can be predicted at any range, the radar's interference robustness, and the use of SMA in FDA MIMO radar.

## References

- [1] Antonik, P.: An investigation of a frequency diverse array. Antonik, P. (2009) An investigation of a frequency diverse array. Doctoral thesis, UCL (University College London) (2009)
- [2] Wang, Y., Zhu, S.: Main-Beam Range Deceptive Jamming Suppression With Simulated Annealing FDA-MIMO Radar. *IEEE Sensors Journal* 20(16), 9056–9070 (2020). DOI 10.1109/JSEN.2020.2982194
- [3] Bang, H., Jian, J., Basit, A., Gui, R., Wang, W.Q.: Adaptive distributed target detection for fda-mimo radar in gaussian clutter without training data. *IEEE Transactions on Aerospace and Electronic Systems* pp. 1–1 (2022). DOI 10.1109/TAES.2022.3145781
- [4] Ding, Z., Xie, J.: Joint transmit and receive beamforming for cognitive fda-mimo radar with moving target. *IEEE Sensors Journal* 21(18), 20878–20885 (2021). DOI 10.1109/JSEN.2021.3100332
- [5] Eker, T., Demir, S., Hizal, A.: Exploitation of linear frequency modulated continuous waveform (lfmcw) for frequency diverse arrays. *IEEE Transactions on Antennas and Propagation* 61(7), 3546–3553 (2013). DOI 10.1109/TAP.2013.2258393
- [6] Gui, R., Wang, W.Q., Cui, C., So, H.C.: Coherent pulsed-fda radar receiver design with time-variance consideration: Sinr and crb analysis. *IEEE Transactions on Signal Processing* 66(1), 200–214 (2018). DOI 10.1109/TSP.2017.2764860
- [7] Huang, Y., Liao, G., Xu, J., Li, J., Yang, D.: Gmti and parameter estimation for mimo sar system via fast interferometry rpca method. *IEEE Transactions on Geoscience and Remote Sensing* 56(3), 1774–1787 (2018). DOI 10.1109/TGRS.2017.2768243
- [8] Jones, A.M., Rigling, B.D.: Planar frequency diverse array receiver architecture. In: 2012 IEEE Radar Conference, pp. 0145–0150 (2012). DOI 10.1109/RADAR.2012.6212127
- [9] Khan, W., Qureshi, I.M.: Frequency diverse array radar with time-dependent frequency offset. *IEEE Antennas and Wireless Propagation Letters* 13, 758–761 (2014). DOI 10.1109/LAWP.2014.2315215
- [10] Khan, W., Qureshi, I.M., Basit, A., Khan, W.: Range-bins-based mimo frequency diverse array radar with logarithmic frequency offset. *IEEE Antennas and Wireless Propagation Letters* 15, 885–888 (2016). DOI 10.1109/LAWP.2015.2478964
- [11] Khan, W., Qureshi, I.M., Saeed, S.: Frequency diverse array radar with logarithmically increasing frequency offset. *IEEE Antennas and Wireless Propagation Letters* 14, 499–502 (2015). DOI 10.1109/LAWP.2014.2368977
- [12] Li, B., Petropulu, A.P., Trappe, W.: Optimum co-design for spectrum sharing between matrix completion based mimo radars and a mimo communication system. *IEEE Transactions on Signal Processing* 64(17), 4562–4575 (2016). DOI 10.1109/TSP.2016.2569479
- [13] Li, J., Stoica, P.: MIMO radar with colocated antennas. *IEEE Signal Processing Magazine* 24(5), 106–114 (2007). DOI 10.1109/MSP.2007.904812
- [14] Liu, Q., Wang, W., LIANG, D., Wang, X.: Real-valued reweighted  $l_1$  norm minimization method based on data reconstruction in mimo radar. *IEICE Transactions on Communications* E98.B, 2307–2313 (2015). DOI 10.1587/transcom.E98.B.2307
- [15] Liu, Y., Wang, C., Gong, J., Chen, G.: Discrimination of mainlobe deceptive target with meter-wave fda-mimo radar. *IEEE Communications Letters* pp. 1–1 (2022). DOI 10.1109/LCOMM.2022.3155371
- [16] Qin, S., Zhang, Y.D., Amin, M.G.: Multi-target localization using frequency diverse coprime arrays with coprime frequency offsets. In: 2016 IEEE Radar Conference (RadarConf), pp. 1–5 (2016). DOI 10.1109/RADAR.2016.7485154
- [17] Sammartino, P.F., Baker, C.J., Griffiths, H.D.: Frequency diverse mimo techniques for radar. *IEEE Transactions on Aerospace and Electronic Systems* 49(1), 201–222 (2013). DOI 10.1109/TAES.2013.6404099
- [18] Shao, H., Li, J., Chen, H., Wang, W.Q.: Adaptive Frequency Offset Selection in Frequency Diverse Array Radar. *IEEE Antennas and Wireless Propagation Letters* 13, 1405–1408 (2014). DOI 10.1109/LAWP.2014.2340893
- [19] S. Li, H. Chen, M. Wang, A. A. Heidari, and S. Mirjalili, “Slime mould algorithm: A new method for stochastic optimization,” *Future Generation Computer Systems*, vol. 111, pp. 300–323, 2020